Mössbauer characterization of ^{57}Fe dopant ions across the insulator-metal transition in ANi$_{0.98}$Fe$_{0.02}$O$_3$ (A=Nd,Lu) perovskites

Igor Presniakov,[1] Gérard Demazeau,[2] Alexey Baranov,[1] Alexey Sobolev,[1] and Konstantin Pokholok[1]

[1]*Chair of Radiochemistry, Department of Chemistry, Lomonosov University, 119992 Moscow, Russia*

[2]*Institut de Chimie de la Matière Condensée de Bordeaux (ICMCB) UPR-CNRS 9048, 87 Avenue A. Schweitzer, 33608 Pessac Cedex, France*

Mössbauer spectroscopy has been used for following the insulator→metal transition versus temperature in ANiO$_3$ perovskites (NdNi$_{0.98}$^{57}Fe$_{0.02}$O$_3$ and LuNi$_{0.98}$^{57}Fe$_{0.02}$O$_3$). The evolution of the number of ^{57}Fe sites and the isomer-shift value at the transition bring important local information taking into account the role of the different factors (structural, geometrical, and bond covalency). Mössbauer measurements have been made as a function of temperature to study electronic and vibrational behavior of the ^{57}Fe probe atoms in the nickelate structure.

INTRODUCTION

The study of electronic phenomena in solids is an important goal in physics. It is possible to classify the main electronic phenomena in two principal categories: intra-atomic phenomena when only the orbitals of the same atoms are concerned (for example, the change of electronic configuration low spin→high spin) and interatomic phenomena involving different atoms in the lattice (charge transfer, insulator→metal transition, disproportionation).

Perovskite-type oxides containing Jahn-Teller ions such as high-spin Fe^{4+}:$t_{2g}^3e_g^1$ and Mn^{3+}:$t_{2g}^3e_g^1$ or low-spin Ni^{3+}:$t_{2g}^6e_g^1$ attract considerable interest due to their remarkable electronic properties.[1] The electronic configurations with one electron in a twofold-degenerate e_g orbitals introduce a specific instability leading to different phenomena: (i) a cooperative Jahn-Teller effect observed for Mn^{3+}-oxide perovskites,[2] (ii) a charge disproportionation 2Fe^{4+}→Fe^{3+}+Fe^{5+} in ferrates CaFeO$_3$[3] and Ca$_{1-x}$La$_x$FeO$_3$[4] with a second- (or higher-) order phase transition from the orthorhombic charge-delocalized state (Fe^{4+}) to the monoclinic charge-disproportionated state (with two iron sites Fe^{3+}/Fe^{5+}) beginning below T_t.[5]

Due to the low-spin configuration of Ni^{3+} in oxygen lattices ($t_{2g}^6e_g^1$), the ANiO$_3$(A=Nd→Lu;Y) perovskites first prepared in 1971 by Demazeau *et al.*[6] are an important model for studying the above electronic phenomena. The structural distortion of the perovskite lattice ANiO$_3$ plays a key role on the localization of the e_g^1 electron and consequently two different factors being involved: (i) the ionic radius of A^{3+} cations along the whole series (La^{3+}→Lu^{3+}) and (ii) the temperature for a constant A^{3+} cation.

The increase of the structural distortion from La^{3+} to Lu^{3+} induces for the smallest rare-earth (Ho→Lu)[7] and Y,[8] Tl[9] cations a partial charge disproportionation 2Ni^{3+}→Ni$^{(3+\alpha)+}$+Ni$^{(3-\alpha)+}$ observed first through high-resolution neutron diffraction through a phase transition: orthorhombic *Pbnm* →monoclinic $P2_1/n$. On the other hand, for a constant ANiO$_3$ composition a thermally driven insulator-metal (*MI*) transition at a T_{IM}[10] and a transition to an unusual long-range antiferromagnetic order below a $T_N(A$=Pr,Nd) or $T_N < T_{MI}(A$=Sm→Lu,Y) have been detected.[11,12]

As the main characterizations of these phenomena are based on structural or magnetic studies—both involving macroscopic characterizations—the objective of our work is to develop Mössbauer spectroscopy as a local characterization. Recently, Mössbauer investigation of the ^{57}Fe-doped nickelates ANi$_{0.98}$Fe$_{0.02}$O$_3$ (A=Lu, Y, Tl) has provided independent evidence for the existence of two different nickel sites.[13,14] The ^{57}Fe spectra of these nickelates were described as a superposition of two subspectra, which indicate that the ^{57}Fe probe atoms are stabilized in two nonequivalent crystallographic positions. On the other hand, the ^{57}Fe spectra of large rare-earth nickelates A=Pr, Nd, Sm showed the existence of only one nickel chemical species, thus underlying the absence of any disproportionation process for the Ni^{III}O$_6$ subarray. In the magnetic ordering domain ($T < T_N$), the ^{57}Fe spectra are resolved into two magnetic sextets with the same isomer shift but considerably different magnetic hyperfine fields.[15] On the base of d_{x2-y2}/d_{z2}—orbital ordering model of Ni^{3+}:$t_{2g}^6e_g^1$ cations, such a particular magnetic environment of Fe^{3+} cations located in the same crystallographic sites has been attributed to the unusual magnetic ordering in ANiO$_3$ (Pr, Nd, Sm) caused by the presence of magnetic frustrated interactions.[15]

In this paper we report results of ^{57}Fe Mössbauer investigations both above and below the metal-insulator transition for the two types nickelates: NdNi$_{0.98}$Fe$_{0.02}$O$_3$ having T_{MI} coinciding with the paramagnetic-antiferromagnetic transition (T_N) and LuNi$_{0.98}$Fe$_{0.02}$O$_3$ for which T_N is lower than T_{MI}, leading to the existence of an intermediate regime $T_N \leqslant T \leqslant T_{MI}$, with the insulating and paramagnetic state. Mössbauer measurements have been made as a function of temperature to study electronic and vibrational behavior of the ^{57}Fe probe atoms in the nickelate structure.

EXPERIMENT

NdNi$_{0.98}$Fe$_{0.02}$O$_3$ sample was prepared by the high oxygen pressure treatment of precursors obtained from sol-gel

method. Appropriate amounts of Nd_2O_3, $Ni(NO_3)_2 \cdot 6H_2O$, ^{57}Fe metal, and citric acid were dissolved in dilute nitric acid. Then, the solution was evaporated while maintaining a pH of 5–6 until a gel was formed. This gel was decomposed at 750 °C in air. At the last stage, the homogeneous precursor mixture was annealed for several days at 850 °C and at an oxygen pressure of 100 MPa.

The synthesis of $LuNi_{0.98}Fe_{0.02}O_3$ sample involved two stages. In the first stage, nickel and iron hydroxides were coprecipitated by a 3M KOH solution from an acid solution of a stoichiometric mixture of Ni(II) and ^{57}Fe(III) salts. The homogeneous hydroxide mixture was washed, dried, and annealed in air at 300 °C until the formation of ^{57}Fe-doped $Ni_{0.98}Fe_{0.02}O$ oxide. At the second stage, a stoichiometric mixture of Lu_2O_3 and $Ni_{0.98}Fe_{0.02}O$ (with the addition of a small amount of $KClO_3$) was annealed in a gold capsule at 900 °C and 6 GPa.

Powder x-ray-diffraction profiles were recorded on a Philips PW 1050 diffractometer using graphite-monochromated Cu-$K\alpha$ radiation. X-ray diffraction diagrams for Nd and Lu samples have been analyzed in the space group *Pbnm*. No additional peaks, which could indicate the presence of superstructures or departure from the mentioned symmetry, were observed in any of the examined diagrams.

dc magnetic susceptibility was measured using a SQUID magnetometer (Quantum Desing MPMS) in the temperature range 5–300 K at 10 000 G after zero-field cooling. The ^{57}Fe-doped $NdNi_{0.98}Fe_{0.02}O_3$ sample shows lower value of $T_N=150$ K than that for undoped $NdNiO_3$ nickelate (200 K).[11] One of the possible reasons for the effect of small amounts of the paramagnetic iron impurity on T_N can be associated with the perturbation of Ni^{3+}-O-Ni^{3+} couplings by Fe^{3+} cations.[15]

The ^{57}Fe Mössbauer spectra were recorded at various temperatures using a conventional constant acceleration Mössbauer spectrometer. The radiation source ^{57}Co(Rh) was kept at room temperature. All isomer shifts refer to the α-Fe absorber at 300 K.

RESULTS AND DISCUSSION

$NdNi_{0.98}Fe_{0.02}O_3$

All the ^{57}Fe Mössbauer spectra of $NdNi_{0.98}Fe_{0.02}O_3$, recorded over the temperature range $[T>T_{IM}(=T_N)]$, were this nickelate is paramagnetic metal, can be described as a single quadrupole doublet (Fig. 1). The small value of the quadrupole splitting $\Delta=0.06\pm0.01$ mm/s indicates that substitutional iron cations are located in sites with the high symmetry of the nearest anionic surrounding, thus underlining the nearly regular NiO_6 octahedra in the first members of the $ANiO_3$ family ($A=$Pr, Nd, Sm).[7,16]

The isomer shift (IS) $\delta=0.22\pm0.01$ mm/s (300 K) for the $NdNi_{0.98}Fe_{0.02}O_3$ spectrum is found to be significantly smaller than $\delta=0.37$ mm/s observed early for the high-spin $Fe^{3+}:t_{2g}^3 e_g^2$ cations in the $NdFeO_3$ orthoferrite with the same orthorhombic structure.[17] Such a difference could be attributed to the increase of the iron valency from "3+" to "4+" due to the electron-transfer reaction
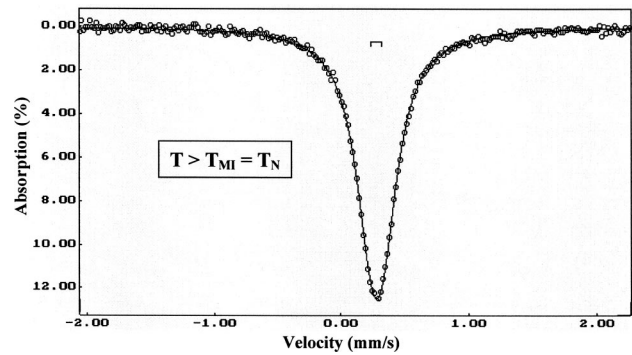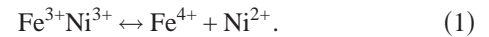

FIG. 1. ^{57}Fe Mössbauer spectrum of $NdNi_{0.98}Fe_{0.02}O_3$ at 300 K.

$$Fe^{3+}Ni^{3+} \leftrightarrow Fe^{4+} + Ni^{2+}. \qquad (1)$$

Since the $Fe^{4+/3+}:3d^5$ redox level is known to be at least 1 eV below the $Ni^{3+/2+}:3d^8$ redox couple in oxides[18] as illustrated schematically in Fig. 2, the equilibrium of the charge-transfer reaction (1) is biased strongly to the left, thus stabilizing formally trivalent Fe^{3+} ions. Therefore, the decrease of the IS value cannot be attributed to the stabilization of tetravalent Fe^{4+} cations.

Taking into account that the ^{57}Fe valence is equal to 3+, two different factors can influence the IS value: (i) a chemi-
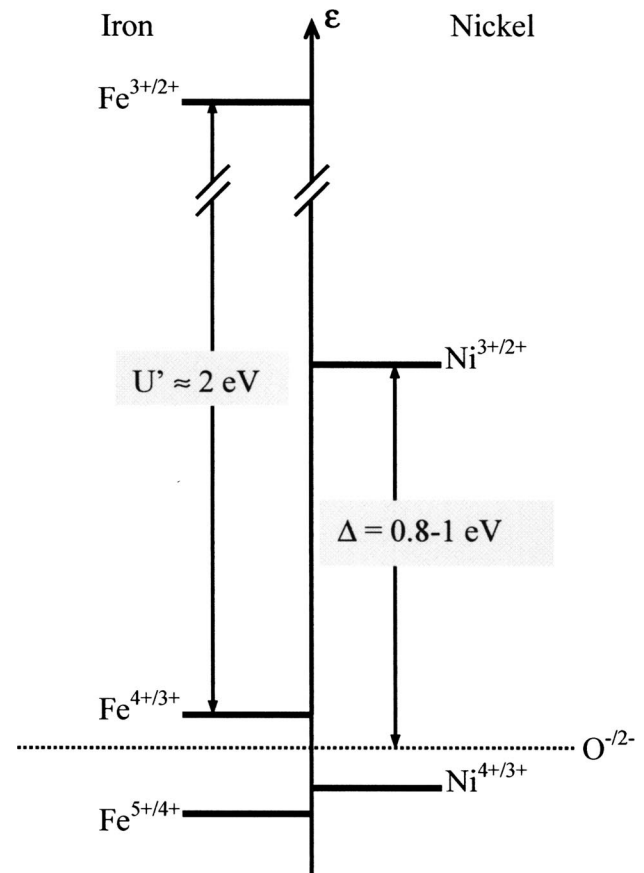

FIG. 2. Semiempirical impurity-level scheme for Fe^{n+} and Ni^{n+} ions in oxides.

cal one, including the covalency of the Fe^{3+}-O chemical bond directly correlated to the competition with the Ni^{3+}-O bond (inductive effect)[19] and (ii) a geometric one corresponding to the Fe^{3+}-O distance in the $NdNiO_3$ lattice.

According to independent measurements of the ESR spectra of TiO_2:Fe and TiO_2:Ni,[20] the substitutional iron impurities would have the $Fe^{4+/3+}$ redox energy some 0.5 eV above the narrow $Ni^{4+/3+}$:$3d^7$ band as a result of the smaller effective nuclear charge experienced by $3d$ electrons on the lighter iron atoms. The result is an increase of the ionicity of the Fe^{3+}-O bonding along the Fe^{3+}-O-Ni^{3+} bonds due to the presence of more covalent competing Ni^{3+}-O bonding, which should decrease a population of iron $4s$ orbitals, and thus increase the IS value.[19] However, this prediction contradicts with the observed decreasing of the IS value for Fe^{3+} cations in ANi$_{0.98}$Fe$_{0.02}$O$_3$ samples as compared to IS value in iron oxides. Therefore, the inductive effect introduced by the competition between the covalent Ni^{3+}-O bonds and Fe^{3+}-O cannot explain the change of the IS value for trivalent iron cations in the nickelate matrix.

Another mechanism is related to the overlap of the iron inner ns-shells ($n=1-3$) with oxygen $2p_\sigma$ wave functions which produces a significant change in s-electron density $\rho_s(0)$ at the iron nucleus. This mechanism, called the overlap distortion effect,[21] is a consequence of the Pauli exclusion principle which forces the electrons to keep out of the overlap region enhancing $\rho_s(0)$ value (reducing IS value). Taking into account that the ^{57}Fe doping into the $NdNiO_3$ matrix introduces a shrinking of the Fe-O distances ($r_{Ni3+} \approx 0.54$ Å, $r_{Fe3+} \approx 0.63$ Å),[22] the overlap distortion effect would play the main contribution on the observed decrease of the IS value.

In order to obtain an evaluation of the influence of the bond-length change IS value, we estimated the change in charge density $\Delta\rho_{ov}(0)$ produced by this distance reduction on account of the overlap distortion effect. It was demonstrated by Simanek *et al.*[21] that overlap distortion of the iron ns orbitals in ionic compounds can be obtained using a Schmidt orthogonalization procedure which does not contain any covalency electron transfer effects. In this case, the change in the charge density at iron nucleus in octahedral oxygen coordination is given by

$$\Delta\rho_{ov}(0) = 2\left[\sum_{n=1}^{3} \frac{6}{1+R'} S_{ns}^2 \phi_{ns}^2(0) \right.$$
$$\left. + 2\sum_{n,m=1}^{3} \frac{6}{1+R'} S_{ns} S_{ms} \phi_{ns}(0) \phi_{ms}(0) \right], \quad (2)$$

where $R'(\approx 0.4)$ is the oxygen-oxygen overlap integrals and $S_{ns}=\langle\phi_{ns}|\phi_{2p}\rangle$ are the overlap integrals, which are strongly dependent on the iron-oxygen distance (Table I). We take $\phi_{1s}=73.30$, $\phi_{2s}=-22.21$, and $\phi_{3s}=8.31$ a.u., as given by the computations of Watson for Fe^{3+} cations.[23] By taking into account the overlap effect and the fact that the Fe-O distance in NdNi$_{0.98}$Fe$_{0.02}$O$_3$ is about 7% shorter than that in NdFeO$_3$, we obtain from Eq. (2) an increase in $\Delta\rho_{ov}(0)$ by about $1.34a_0^{-3}$. Using an isomer shift calibration constant $\alpha = \partial IS/\partial\rho_s(0) \approx 0.2$,[24] the value of $\Delta IS=(\delta_{NdFeO_3}-\delta_{NdNiO_3})$

TABLE I. The average Fe-O distances and the values of overlap integrals (S_{ns}) in NdNi$_{0.98}$Fe$_{0.02}$O$_3$ and NdFeO$_3$.

Compounds	$\langle R(\text{Fe-O})\rangle$ Å	S_{1s}	S_{2s}	S_{3s}
NdNi$_{0.98}$Fe$_{0.02}$O$_3$	1.94	0.00314	0.02337	0.11216
NdFeO$_3$	2.03	0.00263	0.01976	0.09575

was found to be 0.19 mm/s. This theoretical value is in agreement with experimental difference IS=0.15 mm/s. It should be noted that, in addition to the overlap distortion, the decrease of Fe-O distance is accompanied by an increase of a population of iron $3d$ and $4s$ orbitals, which influence on the IS value in the wrong direction.[19] It is, however, very difficult to obtain a good quantitative estimate of the relative amount of electron transfer to the $3d$ and $4s$ orbitals and we neglected them in analyzing the above data. Hence, by neglecting the covalency effects, we actually underestimate the increase in $\Delta\rho_0(0)$ with reduction of the Fe-O bond length.

The second part of the discussion is devoted to the discussion of the variation versus temperature of the IS value for $T>T_{MI}$. In the range $T>T_{MI}$, the IS value exhibits the usual increase with the decreasing of temperature (Fig. 3) due to the second-order Doppler shift (δ_{SOD}), which adds to the IS (δ_{el}) depending on the electron density at ^{57}Fe nucleus to give the total measured shift (δ):[19]

$$\delta(T) = \delta_{el} + \delta_{SOD}(T). \quad (3)$$

The observed temperature dependence of IS in the temperature range $100 \leq T \leq 300$ K is well fitted by a linear relationship indicated by the solid line in Fig. 3. The temperature coefficient $\partial\delta/\partial T = -5.2\times10^{-4}$ mm/s K, calculated from the slope of $\delta(T)$ dependence is in agreement with the average slope $\langle\partial\delta/\partial T\rangle = -4.2\times10^{-4}$ mm/s K early obtained for the orthoferrite AFeO$_3$ family (A=rare earths).[17]

From a chemical point of view the temperature dependence of experimental IS value related to the $\delta_{SOD}(T)$ is interesting with respect to its simple relation with a recoil-free fraction (f) and a force constant (K) experienced by Möss-
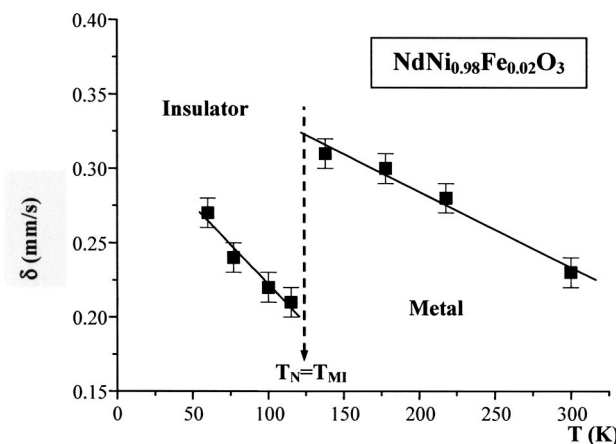

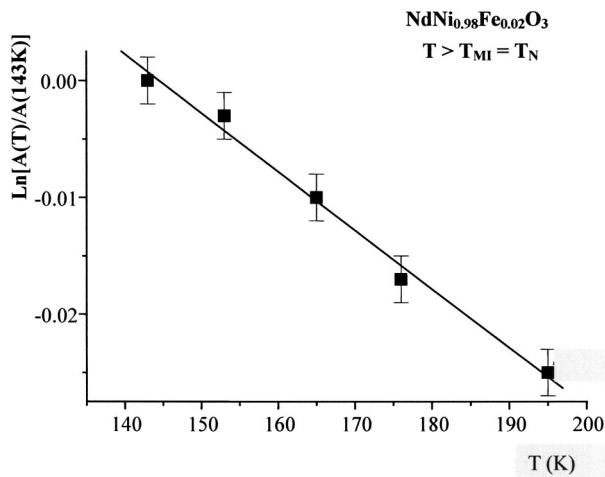FIG. 3. Temperature dependence of the ^{57}Fe isomer shift for NdNi$_{0.98}$Fe$_{0.02}$O$_3$.

FIG. 4. Thermal evolution of the logarithm of the ^{57}Fe normalized absorption area for NdNi$_{0.98}$Fe$_{0.02}$O$_3$

bauer nucleus, which significantly depends on chemical bonding and the local structure of iron cations[25]

$$\frac{\partial \delta_{\mathrm{SOD}}(T)}{\partial T} = \left(\frac{3\hbar^2}{2ME_\gamma^2}K\right)\frac{\partial \ln f(T)}{\partial T}, \qquad (4)$$

where (i) E_γ is the nuclear transition energy for ^{57}Fe nucleus, (ii) M is atomic mass of iron, and (iii) $f(T)$ is the recoil-free fraction (or Debye-Waller factor). In a Debye approximation [n], the temperature dependence of the $f(T)$ is given by the equation

$$\ln f(T) = -\frac{3E_R}{2k_B\Theta_D}\left[1 + 4\left(\frac{T}{\Theta_D}\right)^2\int_0^{\Theta_D/T}\frac{x\,dx}{e^x - 1}\right], \qquad (5)$$

where (i) k_B is the Boltzmann constant, (ii) $E_R = 0.002$ eV is the recoil energy of the free ^{57}Fe nucleus, and (iii) Θ_D is the Debye temperature. At low temperatures ($T \ll \Theta/2$), the zero-phonon fraction is nearly constant, and near Θ_D (high-temperature limit) it shows approximately a linear decrease.

For a thin absorber the temperature of recoil-free fraction is well represented by the temperature dependence of the area (A) under the resonance curve. The thermal evolution of the logarithm of normalized absorption area for ^{57}Fe dopant in NdNi$_{0.98}$Fe$_{0.02}$O$_3$ is shown in Fig. 4. The observed slop of this linear dependence $\partial \ln[A(T)/A(100)]/\partial T = -5.02 \times 10^{-4}$, allows one to determine the Mössbauer lattice temperature (Θ_M) as probed by the ^{57}Fe atoms, using the relationship valid in the high-temperature limit[26]

$$\frac{\partial \ln A(T)}{\partial T} = \frac{\partial \ln f(T)}{\partial T} = -\frac{3E_\gamma^2}{k_BMc^2\Theta_M^2}. \qquad (6)$$

The least squares fitted to experimental points leads to $\Theta_M = 450 \pm 10$ K. This value agrees well with those probed by the ^{57}Fe dopant in other structures of transition metal compounds.[27,28] However, it should be noted that this value is not to be compared with Debye temperatures from independent specific-heat data, because they are determined by different weighted averages over the frequency spectrum.

Substitution of $\partial \ln f(T)/T$, obtained from the temperature dependence of the resonant area (Fig. 4) into Eq. (4), yields the force constant $K = 0.97 \times 10^5$ dyn/sm, experienced by ^{57}Fe probe atoms in NdNi$_{0.98}$Fe$_{0.02}$O$_3$ lattice. This value can be compared to $K = 1.5 \times 10^5$ dyn/sm for NdFeO$_3$,[17] obtained by the same procedure, using the experimental values $\langle \partial \delta/\partial T \rangle = -4.2 \times 10^{-4}$ mm/s K and $\Theta_M = 720$ K [see Eq. (6)]. The observed large difference $\Delta K = 0.53 \times 10^5$ dyn/sm, in the force constant values between iron and oxygen atoms in the two perovskites having the same local environments of ^{57}Fe atoms suggests a very different covalent contribution in the Fe-O bonds in these oxides.

The third part of the discussion is devoted to the analysis of the change of IS value at the transition temperature. Around $T \approx T_{MI}(=T_N)$, the IS value undergoes an abrupt decrease and the slope of the thermal dependence for $\delta(T)$ also shows a significant change (Fig. 3). Since the experimentally derived IS is the sum of a term depending on the electron density at ^{57}Fe nucleus (δ_{el}) and of the temperature-dependent second-order Doppler shift δ_{SOD} [see Eq. (3)] it is only possible to conclude that either or both are undergoing anomalous change in the vicinity of $T_{MI}=T_N$. However, we supposed that the observed discontinuity in IS ($\Delta\delta = 0.12$ mm/s) could be attributed to the structural anomalies across the *MI* transition in Pr, Nd nickelates,[29] which induce significant electron-density redistribution such that the s-electron density at ^{57}Fe nucleus is enhanced by $\Delta\rho_s(0) \sim 0.6$ a.u. (Ref. 30) in the insulator phase.

In fact, according to neutron-diffraction data for PrNiO$_3$ and NdNiO$_3$, on cooling through T_{IM} its volume expands by $\sim 0.2\%$ due to a slight increase of the average Ni-O distances (~ 0.004 Å) and decrease in the Ni-O-Ni bond angle ($\Delta\theta \approx -0.5°$).[29] We believe the reduced IS for ^{57}Fe^{3+} probe ions in insulator regime ($T > T_{MI}$) reflects an enhanced covalent contribution to Fe-O bonds due to a reduction of the Fe-O-Ni angle which reduces the competition effect for the same O^{2-}:$2p_\sigma$ orbitals by the bridged Fe^{3+} and Ni^{3+} cations. The covalent electron back transfer from the O^{2-}:$2p_\sigma$ to Fe^{3+}:$4s$ orbitals would increases $\rho_{4s}(0)$ charge-density at the iron nucleus and therefore reduces the IS from the value observed $T > T_{MI}$. This change of $\rho_{4s}(0)$ is pronounced enough to overcompensate the some covalent transfer to empty Fe^{3+}:$3d$ orbital, which increases the screening of the core ns electrons ($n = 1-3$) from nuclear charge, thus increasing the IS value. This conclusion is qualitatively consistent with observation that in high-spin Fe^{3+}:$t_{2g}^3 e_g^2$ cations, all $3d$ orbitals are singly occupied so that the net gain energy resulting from electron transfer from the oxygen to these orbitals is not as large as for the empty $4s$ orbitals.

Figure 3 shows the significant change in the slope $\partial\delta(T)/\partial T \approx -8.1 \times 10^{-4}$ mm/s K at $T < T_N(=T_{MI})$. According to Eq. (4), this change can be attributed to a magnetization-dependent Lamb-Mössbauer f factor [or lattice temperature (ΘM), see Eq. (6)] probed by the ^{57}Fe atoms in the nickelate structure. Some authors have observed the same abrupt change below the magnetic ordering temperature of the slope of the curve $f(T)$, which physically means that the mean square displacement of the ^{57}Fe atoms decreases.[31,32] The large increase of the f factor can be related to a strong
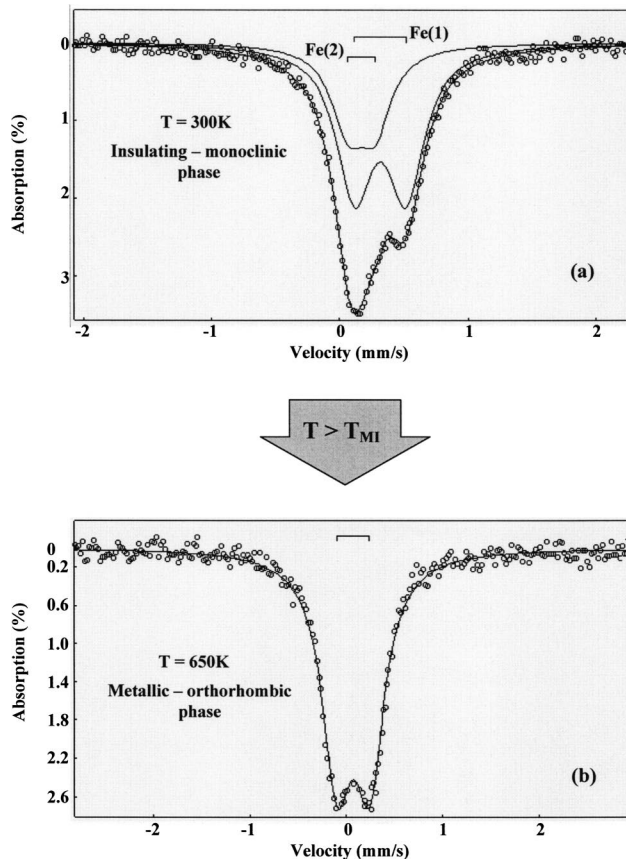
FIG. 5. ^{57}Fe Mössbauer spectra of LuNi$_{0.98}$Fe$_{0.02}$O$_3$ at (a) $T < T_{IM}$ and (b) $T > T_{IM}$.

magnon-phonon coupling (see the works of Eremenko *et al.* cited in Ref. 33), thus underlying the important role of magnetic and electron-lattice interactions as a driving force for the insulator-metal transition.

It should be noted that in a recent Mössbauer study of NdNi$_{0.98}$Fe$_{0.02}$O$_3$ (Ref. 15) at $T < T_{IM}$, the Mössbauer spectra have been resolved into two magnetic Zeeman spectra with the same isomer shift values, and quadrupole splitting which underlined that all the Fe sites are crystallographically equivalent. Only the magnetic hyperfine fields H_1 and H_2 are very different ($H_1 \approx 430-450$ kOe, $H_2 \approx 15-22$ kOe). These results support the orbital ordering in the whole NdNiO$_3$ (Refs. 11 and 12) lattice instead of the charge ordering.[34,35]

LuNi$_{0.98}$Fe$_{0.02}$O$_3$

The ^{57}Fe spectra of LuNi$_{0.98}$Fe$_{0.02}$O$_3$ recorded in the insulator paramagnetic region $T_N < T < T_{IM}$, consist of two quadrupole doublets [Fig. 5(a)] thus indicating that ^{57}Fe dopant are located in two nonequivalent Fe(1) and Fe(2) crystallographic sites. This result is consistent with early observed monoclinic symmetry for the small rare-earth nickelates below T_{IM},[7,16] which implies the existence of two types of alternating Ni(1)O$_6$ and Ni(2)O$_6$ octahedra.

The isomer shifts $\delta_1 = 0.31 \pm 0.01$ mm/s and $\delta_2 = 0.15 \pm 0.01$ mm/s ($T = 300$ K) for both Fe(1) and Fe(2) states fall within the range of δ values corresponding to formally trivalent iron cations in oxide compounds.[19] However, the observed difference between δ_1 and δ_2 values reflects the different covalent character of the Fe-O bonding in Fe(1)O$_6$ and Fe(2)O$_6$ polyhedra. Taking into account that the decrease of the formal oxidation state of iron cations normally leads to the increase of the corresponding isomer shift, the quadrupole doublet with the higher δ_1 value can be assign to the Fe(1) cations substituted for nickel in Ni(1)O$_6$ polyhedra. In this case, the second quadrupole doublet with the smaller δ_2 value should arise from the Fe(2) cations substituted for nickel cations in the electron-enriched Ni(2)O$_6$ polyhedra.

It is very interesting to elucidate how the difference between the formal charges (n_i) of the Fe^{n+}(1) and Fe^{n+}(2) dopant ions, manifesting itself as the difference in corresponding isomer shifts (δ_1 and δ_2), correlates with the charge redistribution (α) between the Ni$^{(3-\alpha)+}$(1) and Ni$^{(3+\alpha)+}$(2) cations caused by the monoclinic distortion of small-earth nickelate lattice. For this purpose, we proposed[14] an empirical expression relating the mean formal charge of high-spin Fe^{n+} cations in octahedral FeO$_6$ polyhedra to the corresponding isomer shift value

$$\delta = (1.25 - 0.30 \times n) \pm 0.03 \,[\text{mm/s}], \qquad (7)$$

where the δ value refers to α-Fe at room temperature and $3 \leqslant n \leqslant 4$ is the mean formal charge of the iron cations on a time scale $\tau > 10^{-8}$ s. Substituting the experimental δ_1 and δ_2 values in the relation (7), the formal valences $n_1 = 3.13$ and $n_2 = 3.67$ for Fe(1) and Fe(2) cations, respectively, were calculated. The effective charge values thus obtained clearly indicate the two chemically different Fe(1) and Fe(2) sites for iron probe atoms. Moreover, the difference between these values $\Delta n = 0.54$ is consistent with the difference $\Delta n = 0.66$ between the formal valences for Ni^{n+}(1) (2.58) and Ni^{n+}(2) (3.24) ions in LuNiO$_3$ calculated using bond-valence Brown's model.[16] This finding provides independent quantitative evidence for a charge disproportionation phenomenon associated with the insulating phase of LuNiO$_3$ perovskite.

It should be noted that the ratio of the areas $A(1)/A(2) \approx 2$ under the Fe(1) and Fe(2) sub-spectra considerably differs from unity and therefore indicates the lack of random distribution of dopant iron cations over two crystallographic positions in the monoclinic lattice of LuNi$_{0.98}$Fe$_{0.02}$O$_3$. A reason for this can be "steric" effects caused by the fact that average iron-oxygen distances in trivalent iron oxides $\langle$Fe^{3+}-O$\rangle = 2.03$ Å,[22] are close to that in Ni(1)O$_6$ polyhedra in the monoclinic LuNi$_{0.98}$Fe$_{0.02}$O$_3$ structure, $\langle$Ni(1)-O$\rangle = 2.00$ Å.[16] This seems to result in the preferable substitution of trivalent iron for Ni(1) cations rather than for Ni(2) cations located in considerably smaller Ni(2)O$_6$ polyhedra, $\langle$Ni(2)-O$\rangle = 1.92$ Å.[12] Moreover, in our previous work[13,14] it has been found that the $A(1)/A(2)$ ratio remains constant within the experimental error for ANi$_{0.98}$Fe$_{0.02}$O$_3$ ($A =$ Lu, Y, Tl) nickelates with a varied degree of monoclinic distortion. This finding is qualitatively consistent with the data of Alonso *et al.*[33] who showed that the effective charge of the Ni(1) and Ni(2) cations and, hence, the sizes of the Ni(1)O$_6$ and Ni(2)O$_6$ polyhedra, respectively, remain unal-
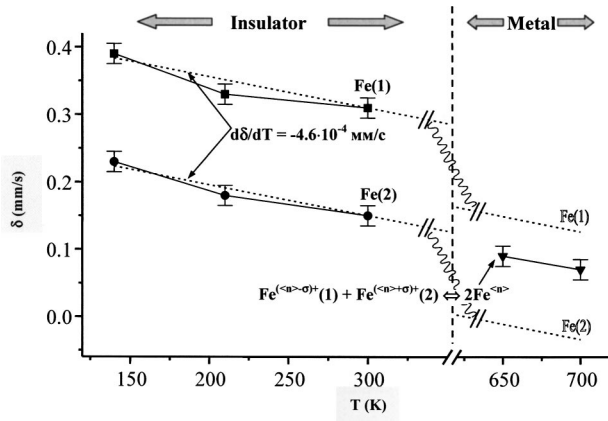
FIG. 6. Temperature dependence of the ^{57}Fe isomer shift for Fe (1) and Fe (2) subspectra for LuNi$_{0.98}$Fe$_{0.02}$O$_3$. The dashed lines are calculated from the average slope $\partial\delta/\partial T = -4.6\times10^{-4}$ mm/s K (see text).

FIG. 7. Schematics of the change in the local environment of Fe^{3+} ions upon the monoclinic-orthorhombic transition of LuNi$_{0.98}$Fe$_{0.02}$O$_3$ structure.

tered while the degree of monoclinic distortion increases in ANiO$_3$ nickelates series (Ho→Lu, Y).

The analysis of the temperature-dependent ^{57}Fe Mössbauer data (δ,Δ) has allowed us to follow the structural changes of the local environments of iron dopant ions concomitant with the electronic delocalization in the NiO$_6$ subarray as the LuNi$_{0.98}$Fe$_{0.02}$O$_3$ sample is heated through the insulator-metal transition. Figure 6 shows the thermal dependence of δ_1 and δ_2, which are very sensitive to the electronic state of Fe(1) and Fe(2) ions, respectively. In the temperature range $T_N \lesssim T \lesssim T_{IM}$, the δ_1 and δ_2 values decrease monotonically upon increasing temperature with the slope $\partial\delta/\partial T \approx -0.48\times10^{-4}$ mm/s, which can be related to the second-order Doppler effect. It suggests a very weak (if any) thermal dependence of effective charge for the iron dopant cations in the Fe(1)O$_6$ and Fe(2)O$_6$ polyhedra. This conclusion is very consistent with the recent high-resolution neutron data for undoped LuNiO$_3$,[36] in which the degree of charge disproportionation (σ) of Ni$^{(3-\alpha)+}$(1) and Ni$^{(3+\alpha)+}$(2) cations, defined by the size difference between large, Ni(1)O$_6$, and small, Ni(2)O$_6$, polyhedra, reaches a maximum already at room temperature.

One of the main findings is that upon heating of LuNi$_{0.98}$Fe$_{0.02}$O$_3$ sample well above T_{IM}, the ^{57}Fe spectrum shows the abrupt convergence of the two Fe(1) and Fe(2) subspectra, in the monoclinic-insulating phase, to one quadrupole doublet in the orthorhombic-metallic phase [Fig. 5(b)]. This result would suggest the formation of a unique state for iron probe atoms and could, therefore, imply that the charge disproportionation in NiO$_6$ subarray completely vanishes at the *MI* transition.

The isomer shift value $\delta=0.08\pm0.02$ mm/s (653 K), corresponding to a single Fe$^{\langle n\rangle+}$ site in the high-temperature orthorhombic phase, is intermediate between those determined by extrapolation of the $\delta_1(T)$ and $\delta_2(T)$ curves in the insulating-monoclinic phase if no electronic effects were present at T_{MI} (Fig. 6). We supposed that upon the monoclinic distortion, the Fe(1) dopant cations substituted for nickel cations in the octahedral Ni(1)O$_6$ sites with a larg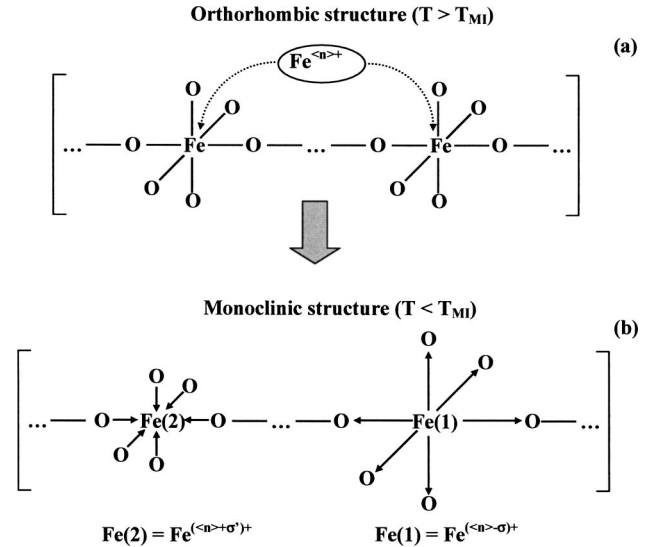er volume will decrease their formal positive charge with respect to the reference Fe$^{\langle n\rangle+}$ state by σ, i.e., Fe$^{(\langle n\rangle-\sigma)+}O_6$ (Fig. 7). Therefore, the Fe(2) cations substituted for nickel in the smaller Ni(2)O$_6$ polyhedra will increase their charge by σ, i.e., Fe$^{(\langle n\rangle+\sigma)+}O_6$. Substitution of $\delta_{298\ K}=0.23$ mm/s, calculated by correction of the $\delta_{653\ K}=0.08\pm0.02$ value for the second-order Doppler shift $\delta_{298\ K}=\delta_{650\ K}+\partial\delta/\partial T\times\Delta T$, into Eq. (7), yields the formal effective charge $\langle n\rangle=3.40$. Using this value, the changes in the effective charges $\sigma=|\langle n\rangle-n|$ were calculated for the Fe(1): $\sigma_1=0.27$ and Fe(2): $\sigma_2=0.26$ with respect to the reference Fe$^{\langle n\rangle+}$ site.

An interesting point is the σ_1 and σ_2 values obtained using the above empirical formula (7) appear to be in good agreement with the degree of charge disproportionation, $\alpha=|\langle n\rangle-n|$, for the two nickel sites Ni(1): $\alpha_1=0.32$ and Ni(2): $\alpha_2=0.34$, in the monoclinic-insulating phase defined with respect to the single Ni$^{\langle n\rangle+}$ sites with $\langle n\rangle=2.90$ in the orthorhombic-metallic phase. We are thus led to conclude that the charge state and the local environment of ^{57}Fe probe atoms are very sensitive to the variation of electronic structure in the NiO$_6$ subarray of LuNi$_{0.98}$Fe$_{0.02}$O$_3$ nickelate. Taking into account the very different electronic configurations and chemical properties of trivalent Ni^{3+} and Fe^{3+} cations, this result is very surprising. Calculations of the ^{57}Fe doped nickelate electronic structure in the local-density approximation +U approach are under investigation to confirm our results.

[1] M. Imada, A. Fujimori, and Y. Tokura, Rev. Mod. Phys. **70**, 1039 (1998).

[2] J. B. Goodenough, Phys. Rev. **100**, 564 (1955).

[3] T. Takeda, R. Kanno, Y. Kawamoto, M. Takano, S. Kawasaki, T. Kamiyama, and F. Izumi, Solid State Sci. **2**, 673 (2000).

[4] S. Komornicki, L. Fournes, J.-C. Grenier, F. Menil, M. Pouchard, and P. Hagenmuller, Mater. Res. Bull. **16**, 967 (1981).

[5] P. M. Woodward, D. E. Cox, E. Moshopoulou, A. V. Sleight, and S. Morimoto, Phys. Rev. B **62**, 844 (2000).

[6] G. Demazeau, A. Marbeuf, M. Pouchard, and P. Hagenmuller, J. Solid State Chem. **3**, 582 (1971).

[7] J. A. Alonso, M. J. Martinez-Lope, M. T. Casais, M. A. G. Aranda, and M. T. Fernandez-Diaz, J. Am. Chem. Soc. **121**, 4754 (1999).

[8] J. A. Alonso, J. L. Garsia-Munoz, M. T. Fernandez-Diaz, M. A. G. Aranda, M. J. Martinez-Lope, and M. T. Casais, Phys. Rev. Lett. **82**, 3871 (1999).

[9] S.-J. Kim, M. J. Martinez-Lope, M. T. Fernandez-Diaz, J. A. Alonso, I. A. Presniakov, and G. Demazeau, Chem. Mater. **14**, 4926 (2002).

[10] J. B. Torrance, P. Laccore, A. I. Nazzal, E. J. Ansaldo, and Ch. Niedermayer, Phys. Rev. B **45**, 8209 (1992).

[11] J. L. Garsia-Munoz, J. Rodriguez-Carvajal, and P. Laccore, Phys. Rev. B **50**, 978 (1994).

[12] J. Rodriguez-Carvajal, S. Rosenkranz, M. Medarde, P. Laccore, M. T. Fernandez-Diaz, F. Fauth, and V. Trounov, Phys. Rev. B **57**, 456 (1998).

[13] S. J. Kim, G. Demazeau, I. A. Presniakov, K. V. Pokholok, A. V. Sobolev, and N. S. Ovanesyan, J. Am. Chem. Soc. **123**, 8127 (2001).

[14] S. J. Kim, I. A. Presniakov, G. Demazeau, K. V. Pokholok, A. V. Baranov, A. V. Sobolev, D. A. Pankratov, and N. S. Ovanesyan, J. Solid State Chem. **168**, 126 (2002).

[15] S. J. Kim, G. Demazeau, I. A. Presniakov, K. V. Pokholok, A. V. Baranov, A. V. Sobolev, D. A. Pankratov, and N. S. Ovanesyan, Phys. Rev. B **66**, 014427 (2002).

[16] J. L. Garsia-Munoz, P. Laccore, and R. Cywinski, Phys. Rev. B **51**, 15 197 (1995).

[17] M. Eibschutz, S. Shtrikman, and D. Treves, Phys. Rev. **156**, 562 (1967).

[18] K. Mizushima, M. Tanaka, and S. Iida, J. Phys. Soc. Jpn. **32**, 1519 (1972).

[19] F. Menil, J. Phys. Chem. Solids **46**, 763 (1985).

[20] K. Mizushima, M. Tanaka, A. Asai, S. Iida, and J. B. Goodenough, J. Phys. Chem. Solids **40**, 1129 (1979).

[21] E. Simanek and Z. Sroubek, Phys. Rev. **163**, 275 (1967).

[22] R. D. Shannon and C. T. Prewitt, Acta Crystallogr., Sect. B: Struct. Crystallogr. Cryst. Chem. **25**, 925 (1969).

[23] R. E. Watson, Phys. Rev. **111**, 1108 (1958).

[24] J. Danon, in *Application of the Mossbauer Effect* (1966), Ser. No. 50, p. 89.

[25] G. P. Gupta and K. C. Lal, Phys. Status Solidi B **51**, 233 (1972).

[26] R. Dean Taylor and P. P. Craig, Phys. Rev. **175**, 782 (1968).

[27] Th. Sinnemann, R. Job, and M. Rosenberg, Phys. Rev. B **45**, 4941 (1992).

[28] C. W. Kimball, J. L. Matykiewicz, H. Lee, J. Giapintzakis, A. E. Dwight, B. D. Dunlap, J. D. Jorgensen, B. V. Weal, and F. A. Fradin, Physica C **156**, 547 (1988).

[29] J. L. Garsia-Munoz, J. Rodriguez-Carvajal, P. Laccore, and J. B. Torrance, Phys. Rev. B **46**, 4414 (1992).

[30] R. Ingalls, A. Van der Woude, and G. A. Sawatzky, in *Mössbauer Isomer Shifts*, edited by G. K. Shenoy and F. E. Wagner (North-Holland, Amsterdam, 1978), Chap. 7.

[31] J. M. D. Coey, G. A. Sawatsky, and A. H. Morrish, Phys. Rev. **184**, 334 (1969).

[32] G. K. Wertheim, D. N. E. Buchanan, and H. J. Guggenheim, Phys. Rev. B **2**, 1392 (1970).

[33] V. V. Eremenko, N. E. Kaner, and V. D. Chercherskii, Pis'ma Zh. Eksp. Teor. Fiz. **94**, 241 (1988) [Sov. Phys. JETP **67**, 2093 (1988)].

[34] T. Mizokawa, D. I. Khomskii, and G. A. Sawatzky, Phys. Rev. B **61**, 11 263 (2000).

[35] U. Staub, G. I. Meijer, F. Fauth, R. Allenspach, J. G. Bednoz, J. Karpinski, S. M. Kazakov, L. Paolasini, and F. D'Acapito, Phys. Rev. Lett. **88**, 126402 (2002).

[36] J. A. Alonso, M. J. Martinez-Lope, M. T. Casais, J. L. Garsia-Munoz, M. T. Fernandez-Diaz, and M. A. G. Aranda, Phys. Rev. B **64**, 094102 (2001).